RESEARCH REPORTS
Biomaterials & Bioengineering

X. Chen[1]*, T.C. Chadwick[2], R.M. Wilson[3], R. Hill[4], and M.J. Cattell[1]

[1]Centre of Adult Oral Health, Queen Mary University of London, Barts and The London School of Medicine and Dentistry, Institute of Dentistry, Turner Street, London, E1 2AD, UK; [2]496 Alegre Avenue, Nipomo, CA 93444, USA; [3]School of Engineering and Materials Science, Queen Mary University of London, Mile End Road, E1 4NS, UK; and [4]Dental Physical Sciences, Queen Mary University of London, Barts and The London School of Medicine and Dentistry, Institute of Dentistry, Mile End Road, E1 4NS, UK; *corresponding author, xiaohui.chen@qmul.ac.uk

J Dent Res X(X):xx-xx, XXXX

Crystallization of High-strength Fine-sized Leucite Glass-ceramics

ABSTRACT

Manufacturing of leucite glass-ceramics often leads to materials with inhomogeneous microstructures. Crystal-glass thermal mismatches which produce microcracking around larger crystals-agglomerates are associated with reduced mechanical properties. The hypotheses were that fine (< 1 μm) crystal size and uniform microstructure in a thermally matched glass would increase the biaxial flexural strength (BFS). Glass was synthesized, attritor-milled, and heat-treated. Glasses and glass-ceramics were characterized by XRD, SEM, and Dilatometry. Experimental (A, M1A and M2A) and commercial glass-ceramics were tested by the BFS test. Experimental glass-ceramics showed an increased leucite crystal number and decreased crystal size with glass particle size reduction. Leucite glass-ceramics (< 1 μm) showed minimal matrix microcracking and BFS values of [mean (SD) MPa]: M1A = 253.8 (53.3); and M2A = 219.5 (54.1). Glass-ceramics M1A and M2A had higher mean BFS and characteristic strength than the IPS Empress Esthetic glass-ceramic ($p < 0.05$). Fine-grained, translucent leucite glass-ceramics were synthesized and produced high mean BFS.

KEY WORDS: glass-ceramic, flexural strength, microstructure, crystallization.

DOI: 10.1177/0022034510377795

Received January 25, 2010; Last revision May 24, 2010; Accepted May 24, 2010

INTRODUCTION

Leucite glass-ceramics are widely used in dentistry to produce dental restorations by a variety of fabrication routes (Cattell *et al.*, 2005), making these materials extremely versatile. Methods of manufacturing these materials include the blending of high- and low expansion powdered frits (Weinstein *et al.*, 1962), or of synthetic leucite with glasses (Burk and Burnett, 1978) by fusion methods. The controlled heating of a glass and its surface crystallization has also been used (Höland *et al.*, 2003), although not optimized. Commercial production methods produce glass-ceramics with up to 45% leucite volume fraction (Cattell *et al.*, 2005), and with microstructures that lack homogeneity. Microcracking often results around large, irregular leucite crystals and clusters (≈10 μm), inhomogeneously distributed in a glass matrix (Barreiro *et al.*, 1989). Crystal-matrix microcracking and crystal twinning (Palmer *et al.*, 1988) are associated with a temperature dependent (605-625°C) cubic to tetragonal phase transformation (Mackert, 1988). This is in conjunction with a thermal expansion (TEC) change from 10.1 to 25.1 x 10^{-6} K^{-1} (Rouf *et al.*, 1978) and a reversible 1.2% volume change (Mackert, 1988). These processes can introduce stress-raising flaws or decouple the leucite crystals from the glass matrix (Binns, 1983). This can reduce the elastic-stored strain energy of the thermal expansion anisotropy and deplete tangential compressive stresses around the crystals, which are key to strengthening in feldspathic dental porcelain (Denry *et al.*, 1996). A critical particle size for glass-ceramic microcracking was explained by a Griffith-type energy balance criterion (Davidge and Green, 1968). In agreement with this theory, microcracking was minimized in tetragonal leucite glass-ceramics by a reduction in the mean leucite particle diameter (< 4 μm) (Mackert *et al.*, 2001). This type of fine-grained microstructure can be achieved by fine powder milling and controlled heat treatments (Cattell *et al.*, 2006), because leucite crystallization is surface-nucleated (Höland *et al.*, 1995). Several studies indicated that a reduction in leucite crystal size, uniformity of microstructure, and minimal matrix microcracking produced flexural strength increases up to 160 MPa (Shareef *et al.*, 1994; Cattell *et al.*, 2001). However, flexural strength values of 200-300 MPa have been found in fine-grained (0.1-1 μm) leucite glass-ceramics (Rouf *et al.*, 1978), although the glass opacity and high viscosity limit their processing and use for aesthetic restorations. In the present work, the objectives were to use a more controlled processing and crystallization regimen of a designed glass to produce translucent high-strength (> 200 MPa) leucite glass-ceramics with

fine-grained microstructures. These materials were designed with the objectives of reducing the incidence of restoration fracture, reducing enamel wear (Metzler *et al.*, 1999), and increasing translucency (Beall and Duke, 1969). The hypotheses were that a fine crystal size (< 1 μm) and uniform microstructure in a thermally matched glass were associated with an increased biaxial flexural strength.

MATERIALS & METHODS

Glass/Glass-ceramic Synthesis

The glass batch composition was (mol%): 72.6% SiO_2, 10.7% Al_2O_3, 7.9% K_2O, 2.1% CaO, 0.3% TiO_2, 4.7% Na_2O, 1.1% Li_2O, and 0.5% MgO. The glass batch was heated in an electric kiln (Fredrickson Kiln Co., Alfred, NY, USA) at 10°C/min to 1316°C (7 hours hold), and then the frit was cooled and ground to 125 μm (glass A). Glass A was then wet-ground (distilled water) in an Attritor Mill (Model 1-S Lab Attritor, Union Process, Akron, OH, USA) with 5 mm yttria-stabilized zirconia (YTZ) grinding media (Tosoh Inc., Grove City, OH, USA) at 400 rpm. Glass slurry was withdrawn after 15, 30, 45, 60, 90, and 120 minutes of milling. The 120-minute-milled slurry and the glass A materials were then milled according to the regimens shown in Figure 1a, to produce glasses M1A and M2A. Glasses were heat-treated in a furnace (RHF 1600, Carbolite, Hope Valley, UK) from 23°C at a rate of 10°C/min to 650°C (1 hour hold), then ramped to 1120°C (1 hour hold) and air-quenched.

Glass particle size was measured in a Mastersizer/E particle analyzer (Malvern Instruments, Malvern, Worcestershire, UK). Quantitative elemental analysis of the glass powders was carried out following attritor milling, by inductively coupled plasma mass spectrometry (ICP-MS, Elan 9000, Perkin Elmer, Norwalk, CT, USA).

X-ray Diffraction Analysis

X-ray diffraction (XRD) was carried out on the glasses and glass-ceramics by means of an X'Pert Pro X-ray diffractometer (PANalytical, Almelo, The Netherlands). Flat plate θ/θ geometry and Ni-filtered Cu-Kα radiation (λ_1 = 0.1540598 nm and λ_2 = 0.15444260 nm) were used. Data were continuously collected from 5° to 120° (2θ range) with a step size of 0.0334° and a step time of 200.03 sec. Calibration was carried out using NIST standard reference material 660a (lanthanum hexaboride). The structural model of tetragonal leucite (ICDD: 00-038-1423) was used for phase identification. Crystal strain calculations were performed with the XRD data and Eq. 1 (Cullity and Stock, 2001):

$$\varepsilon_a = \frac{a - a_0}{a_0}, \varepsilon_c = \frac{c - c_0}{c_0} \quad (1)$$

where ε_a and ε_c are the strain of leucite in the *a-axis* and *c-axis*, a and c are the mean unit cell dimensions of tetragonal leucite for the tested glass-ceramics, and a_0 and c_0 are the unit cell dimensions of the reference tetragonal leucite (ICDD: 00-038-1423).

Biaxial Flexural Strength Specimen Preparation

The glass-ceramic powders (A, M1A and M2A) were used to fabricate disc specimens (30 *per* group) by moistening 1.0 g of powder with 0.3 mL of modeling liquid (CH B: 24066, VITA, Bad Säckingen, Germany) and compacting in a cylindrical steel mould with a plunger. Discs were placed in a pre-heated (538°C) porcelain furnace (Multimatt MCII, Dentsply, Konstanz, Germany) and sintered at a rate of 38°C/min to 1040°C for 2 min under vacuum. Specimens were next wet-ground to P1000 grade silicon carbide paper. One simulated stain firing in air from 538°C at a rate of 55°C/min to 780°C without hold and one simulated overglaze firing in air from 538°C at a rate of 55°C/min to 860°C with a 0.3 min hold were then applied.

Thirty IPS Empress Esthetic glass-ceramic (Lot: H22624, ETC2, Ivoclar-Vivadent, Schaan, Liechtenstein) specimens were prepared by sprueing Perspex discs (14 mm x 2 mm) onto muffle bases and investing, pre-heating, and heat-extruding in an Optimal press furnace (Jeneric Pentron, Wallingford, CT, USA) according to the manufacturer's instructions. The investment was removed by sandblasting with 50 μm glass beads (Bracon Ltd., Etchingham, East Sussex, UK) at 1.5 x 10^5 Pa pressure. The specimens were wet-ground to P1000 grade silicon carbide paper on the compressive test surface only and fired in a porcelain furnace (Multimatt MCII, Dentsply) according to the manufacturer's recommended (simulated) firing cycles (2 stain and 2 overglaze firings).

Biaxial Flexural Strength Testing

The biaxial flexural strength was determined using the ball-on-ring test fixture. Disc specimens (14 x 2 mm) were centrally loaded on a 10 mm diameter knife-edge support, *via* a 4 mm diameter spherical ball indenter, at a crosshead speed of 1 mm/min. The BFS was calculated by Eq. 2 (Timoshenko and Woinowsky-Krieger, 1959):

$$\sigma_{max} = \frac{P}{h^2}\left\{(1+\nu)\left[0.485 \times \ln\left(\frac{a}{h}\right) + 0.52\right] + 0.48\right\} \quad (2)$$

where σ_{max} was the maximum tensile stress, P was the load measured at fracture, h was the specimen thickness, a was the radius of the knife-edge support, and ν was a Poisson's ratio of 0.25.

Statistical Analysis

Group means were analyzed by one-way ANOVA and Tukey's multiple-comparison test at $p < 0.05$ (Sigma Stat, version 2.03, SPSS Inc., Chicago, IL, USA). Weibull analysis of the test groups was carried out with WeibullSMITH software (Fulton Findings, Torrance, CA, USA). Weibull ~~m~~ and characteristic strength values were compared for the overlap of their double-sided confidence intervals (95% level) to determine differences.

Secondary Electron Microscopy

Polished and etched (0.1% HF, 60 sec) specimens were gold coated and viewed by scanning electron microscopy (JSM

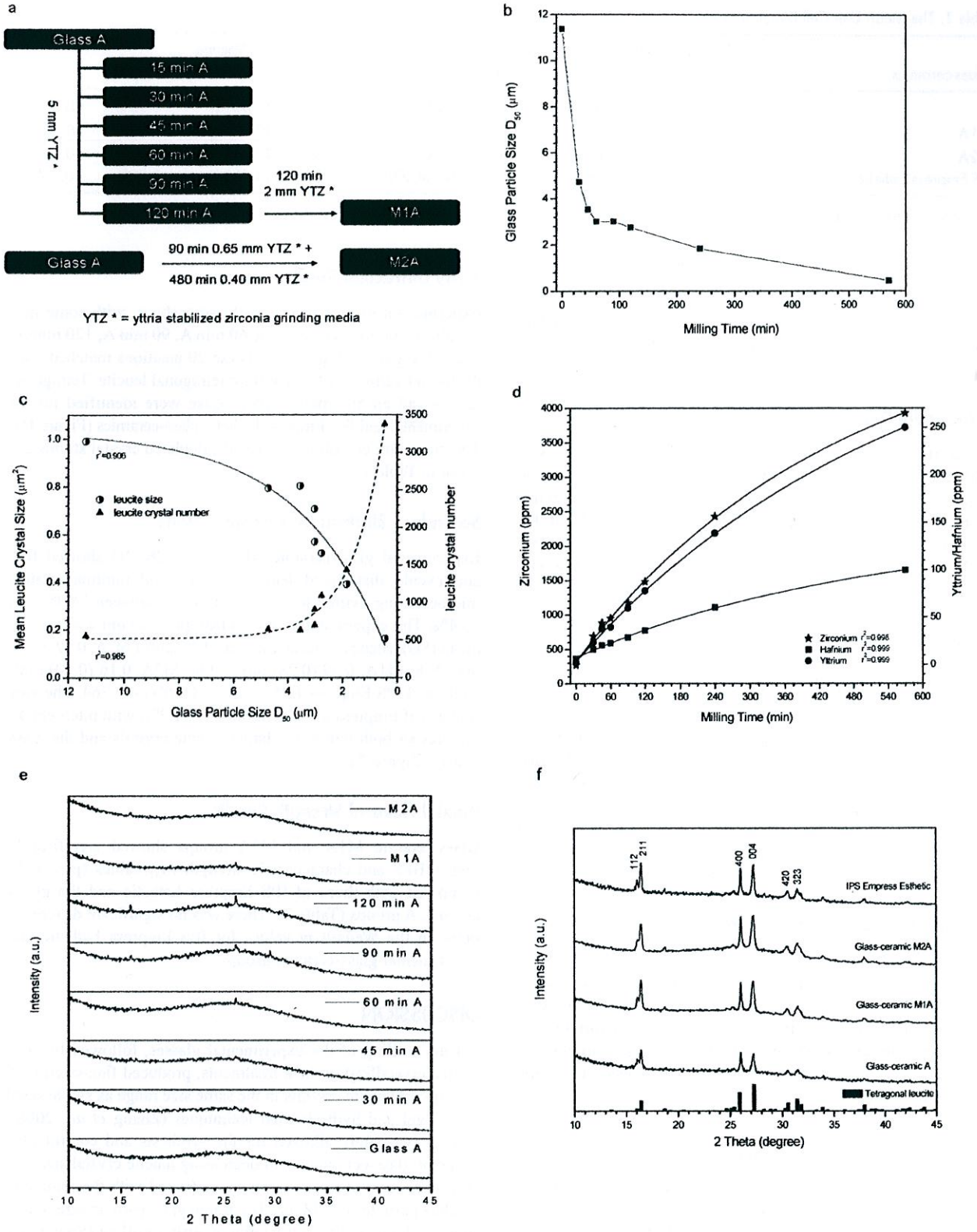

Figure 1. Plots showing the: **(a)** attritor milling regimens for glass A; **(b)** relationship between milling time and particle size of the atttitor-milled glasses A; **(c)** relationship between the mean leucite crystal size, crystal number, and glass particle size of the experimental glass-ceramics; **(d)** relationship between the milling time and zirconium, yttrium, and hafnium content in the attritor-milled glasses A; **(e)** XRD patterns of the attritor-milled glasses; and **(f)** XRD patterns of the glass-ceramics.

Table 1. The Mean Unit Cell Dimensions and Crystal Strains of the Glass-ceramics

Glass-ceramics	Mean *a-axis* Unit Cell Dimension (SD) (nm)	Mean *c-axis* Unit Cell Dimension (SD) (nm)	Mean Unit Cell Volume (SD) (nm^3)	ε_a	ε_c
A	1.31089 (0.00009)	1.37071 (0.00015)	2.35547 (0.0012)	0.33%	–0.35%
M1A	1.31229 (0.00010)	1.36963 (0.00015)	2.35865 (0.0015)	0.44%	–0.43%
M2A	1.31172 (0.00009)	1.36916 (0.00013)	2.35579 (0.0011)	0.40%	–0.46%
IPS Empress Esthetic	1.31069 (0.00006)	1.37170 (0.00009)	2.35645 (0.0032)	0.32%	–0.28%

ε_a = crystal strain in the *a-axis*; ε_c = crystal strain in the *c-axis*.

6300F, JEOL Ltd., Tokyo, Japan). Micrographs (x 2200, area = 2210.4 μm^2) were used to quantify crystal size, number, and area fraction with a light pen (270SD + INT-40, Trackballs, Camarillo, CA, USA) and image analysis software (Sigma Scan Pro 5.0, Systat Software, Inc., Chicago, IL, USA).

Differential Dilatometry

Glass frit was cut into blocks (16 x 6 x 6 mm^3) using a plate saw (Struers Accutom 2, Struers Ltd., Glasgow, Scotland, UK), and glass-ceramic specimens were constructed by either heat extrusion or powder compaction and sintering. The TEC of the specimens were measured by a differential dilatometer (DIL 402PC, Netzsch Instruments, Selb, Germany) at a heating rate of 3°C/min (25 - 1200°C).

RESULTS

Particle Size Analysis Results

The glass particle size (mean D_{50}) *vs.* milling time is shown in Fig. 1b. A decrease in glass particle size [mean D_{50} (SD)] from 11.37 (0.17) to 3.08 (0.04) μm was identified within the first 60-minute milling period. The particle size of glass M1A was 1.79 (0.05) μm, which was further reduced for M2A to 0.45 (0.01) μm. A correlation (exponential fit) between the glass particle size and mean leucite crystal size ($r^2 = 0.906$) and leucite crystal number ($r^2 = 0.985$) was found (Figure 1c).

Inductively Coupled Plasma – Mass Spectrometry Results

Quantitative elemental analysis of the attritor-milled glasses with ICP-MS showed a correlation (polynomial fit) between zirconium ($r^2 = 0.998$), yttrium ($r^2 = 0.999$), and hafnium ($r^2 = 0.999$) content and milling time (Figure 1d). Trace amounts of chromium (70 ppm), nickel (20 ppm), and tungsten (22 ppm) were also found in the glass M2A.

Differential Dilatometry Results

Glass M1A showed a TEC value of 8.5 x 10^{-6} K^{-1}. The TEC and glass transition temperature (T_g) of the glass-ceramics were: A (19.0 x 10^{-6} K^{-1}, 579.1°C), M1A (18.2 x 10^{-6} K^{-1}, 589.5°C), and M2A (17.2 x 10^{-6} K^{-1}, 589.3°C). A lower TEC value of 16.7 x 10^{-6} K^{-1} and a higher T_g of 616.3°C were found for the IPS Empress Esthetic glass-ceramic.

X-ray Diffraction Results

Experimental glasses were largely amorphous, with some tiny visible crystalline peaks for the 60 min A, 90 min A, 120 min A, and M1A glasses (Figure 1e). These 2θ positions matched with the hkl reflections 112 and 400 for tetragonal leucite. Tetragonal leucite and an amorphous glass phase were identified for all experimental and IPS Empress Esthetic glass-ceramics (Figure 1f). The mean unit cell dimensions and calculated crystal strains are given in Table 1.

Secondary Electron Microscopy Results

Experimental glass-ceramics (Figure 2a, 2b, 2c) showed fine and evenly distributed leucite crystals and minimal matrix microcracking, with a leucite area fraction between 24.9% and 25.4%. The experimental and control glass-ceramics showed a mean (SD) leucite crystal size and crystal number of: A, 0.99 (0.59) μm^2, 558; M1A, 0.39 (0.28) μm^2, 1434; M2A, 0.16 (0.10) μm^2, 3378; and IPS Empress Esthetic, 1.72 (1.98) μm^2, 364. The area fraction of Empress glass-ceramic was 31.2%, with microcracking present both within the larger leucite crystals and the glass matrix (Figure 2d).

Biaxial Flexural Strength Results

Glass-ceramic M1A and M2A groups showed significantly higher BFS and characteristic strength (σ_0) values ($p < 0.05$) compared with those of IPS Empress Esthetic and the glass-ceramic A groups (Table 2). There was no significant difference between the Weibull *m* values for IPS Empress Esthetic and experimental glass-ceramic groups.

DISCUSSION

Attritor milling of the experimental glasses, followed by controlled crystallization heat treatments, produced fine-sized 0.16 (0.10) μm^2 leucite crystals in the same size range as synthesized by sol-gel and hydrothermal techniques (Zhang *et al.*, 2008). The present study allowed for the synthesis and control of a range of glass-ceramics with decreasing leucite crystal size and increasing crystal number, which correlated with the reduction of glass particle size (Figure 1c). Rapid glass particle size reduction was found in the first 60 min of attritor milling (Figure 1b), and major reductions were then achieved only with the use of finer grinding media (McLaughlin, 1999). The resultant fine powder sizes achieved increased heterogeneous nucleation sites.

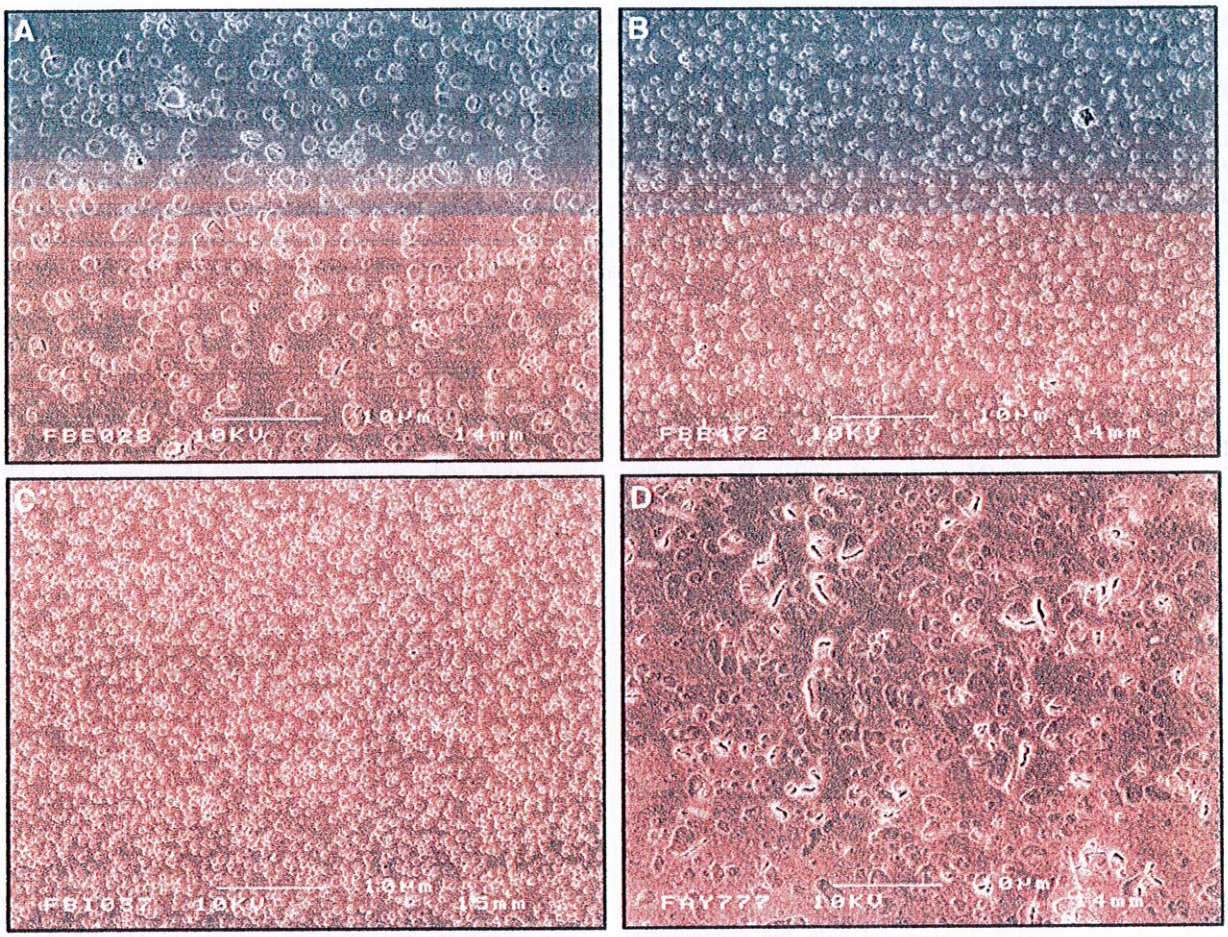

Figure 2. SEM micrographs showing: **(a)** glass-ceramic A, showing uniform leucite crystals (25.0%) and minor crystal microcracking; **(b)** glass-ceramic M1A, showing a uniform dispersal (25.4%) of fine leucite crystals in the glass matrix; **(c)** glass-ceramic M2A, showing an increase of fine leucite crystals (24.9%) and minimal microcracking; and **(d)** IPS Empress Esthetic glass-ceramic, with non-uniform leucite crystal size and matrix-crystal microcracking.

The increased surface area of the glass powder encouraged a large number of sharp edges and a change in particle shape (Müller *et al.*, 2000), and reduced the inhibiting effects of surface elastic strains (Schmelzer *et al.*, 1993). The dramatic increase in crystallite number from 558 to 3378 after sustained milling supports these assumptions. Glass particle size and heat treatments were previously shown to modify crystallization, with the present nucleation step adopted to increase the number of crystallites (Cattell *et al.*, 2006).

The different milling protocols and longer milling times for the M2A glass led to an increase in zirconium, yttrium, hafnium, and other trace elements, associated with the continuous wear of the YTZ grinding media (Figure 1d). The reduction in mean BFS compared with the M1A material could be due to the local agglomeration of these products or the formation of another species and limits this process. Leucite glass-ceramic powder doped with nano-sized (30-60 nm) zirconia (60 wt%) previously produced a bending strength of 214 MPa (Conrad and Meyer, 2007), in the same range as found for the M2A material. When suitably dispersed, zirconia, yttria (> 3 wt%), and hafnia can act as nucleating agents, influencing the viscosity and crystallization kinetics of fine-scale (40-250 nm) glass-ceramics (Rouf *et al.*, 1978; Zheng *et al.*, 2007; Wondraczek and Pradeau, 2008). Trace elements in the M1A glass, if well-dispersed, could encourage the heterogeneous growth of the leucite crystalline phase (James, 1982). Micro- or nano-immiscibility in these glasses is also likely (Cattell *et al.*, 2005), as is the formation of titanates (Rouf *et al.*, 1978). These phases can induce heterogeneous crystallization of a metastable phase, which at increased temperature breaks down into the stable crystalline phase (Pinckney and Beall, 2008). The experimental glasses had some trace crystalline peaks before crystallization heat treatments (Figure 1c). These fine isostructural sites have the potential to reduce the energy barrier for crystallization and provide low-energy crystallization sites (Zhang *et al.*, 2007).

The mean BFS and σ_0 of the experimental glass-ceramics were significantly ($p < 0.05$) increased following milling and crystallization heat treatments (Table 2). This increase in

Table 2. Biaxial Flexural Strength and Weibull Analyses Results of the Tested Glass-ceramics

Glass-ceramics	Mean Flexural Strength (MPa)	SD (MPa)	m	C.I. for m (95%)	σ_0 (MPa)	C.I. for σ_0 (95%)	r^2
A	153.2^a	21.7	8.5^a	6.9 - 10.4	162.0^a	156.0 - 168.2	0.941
M1A	253.8^b	53.3	5.4^{bc}	4.3 - 6.8	274.9^b	259.2 - 291.7	0.971
M2A	219.5^c	54.1	4.7^{bc}	3.8 - 5.8	239.5^c	223.8 - 256.3	0.972
IPS Empress Esthetic	165.5^a	30.6	6.3^{ac}	5.0 - 7.9	177.5^d	168.8 - 186.6	0.977

C.I. = confidence interval, m = Weibull modulus, σ_0 = characteristic strength. Different superscript letters indicate significant differences within categories ($p < 0.05$).

strength was associated with the reduction of leucite crystal size and uniformity of the microstructure. The lack of matrix microcracking at mean leucite crystal sizes of less than 1 μm^2 also supports previous work (Mackert *et al.*, 2001). The homogeneous and fine-scale crystallization could also influence the local depletion of the glass structure, resulting in more favorable residual glass-crystal interfacial stresses. The glass-ceramic M1A had *a-axis* and *c-axis* strains of a similar magnitude (a = 0.44% and c = -0.43%, Table 1), which caused no matrix microcracking and depletion of generated stresses. Changes to the anisotropic stress field and the generation of favorable residual stresses in the glass have been previously linked to strength increases (Denry *et al.*, 1996). Mackert (1988) discussed the presence of microcracks parallel to the *c-axis* in leucite glass-ceramics, partially decoupling crystallites and reducing the bulk thermal expansion. This was evident for the control group, with a reduced *c-axis* strain associated with crystal-matrix microcracking and a lower TEC (16.7 x 10^{-6} K^{-1}, 100-400°C) and mean BFS. A higher area fraction of the high-expansion tetragonal leucite phase (31.2%) compared with the experimental glass-ceramics (24.9-25.4%) also suggests that strain dissipation may have occurred.

Changes to the lattice parameters for the experimental glass-ceramics with glass particle size reduction may be due to changes in glass diffusivity, mobility (Freiman *et al.*, 1971), and crystallization mechanisms (Tošić *et al.*, 2008). The unit cell dimensions (M1A and M2A, Table 1) are also in the same range (a = 1.312-1.315 nm, c = 1.369-1.374 nm) as reported for solid solutions of tetragonal leucite (Hermansson and Carlsson, 1976). A limited substitution of sodium for potassium is possible, and some geological leucites indicate up to 2.4 sodium atoms *per* unit cell (16 $KAlSi_2O_6$ *per* unit cell) (Deer *et al.*, 2004). The incorporation of lithium and sodium into the leucite crystal lattice can cause reduced TEC and modification to the cubic to tetragonal transformation temperature (Ota *et al.*, 1993). The relationship between the transformation temperature, T_g, and glass properties is important to the maintenance of residual stresses and mechanical properties (Lee *et al.*, 1997).

The present study produced leucite glass-ceramics with higher mean flexural strengths (253.8 MPa) than those reported for current leucite glass-ceramics (120-140 MPa) (Höland *et al.*, 2003), and in the same range (200-300 MPa) as reported for an opaque leucite glass-ceramic (Rouf *et al.*, 1978). The original hypothesis can therefore be upheld, because the fine (< 1 μm^2) leucite crystal size and uniformity of microstructure in a thermally matched glass produced high mean biaxial flexural strengths. These new fine-grained leucite glass-ceramics also have other advantages in terms of improved translucency, aesthetics, processability, and reduced enamel wear (Metzler *et al.*, 1999), which will be reported in a future study.

ACKNOWLEDGMENTS

This research was carried out in partial fulfillment for the degree of PhD in the Institute of Dentistry, Barts and The London School of Medicine and Dentistry, 2009. The authors acknowledge Support for Oral Science, Barts and the London, School of Medicine and Dentistry and the Den-Mat Corporation for the support of this research.

REFERENCES

Barreiro MM, Riesgo O, Vicente EE (1989). Phase identification in dental porcelains for ceramo-metallic restorations. *Dent Mater* 5:51-57.

Beall GH, Duke DA (1969). Transparent glass-ceramics. *J Mater Sci* 4:340-352.

Binns D (1983). The chemical and physical properties of dental porcelains. In: *Dental ceramics: proceedings of the First International Symposium on Ceramics*. McLean JW, editor. Chicago: Quintessence Publishing Co., pp. 41-56.

Burk B, Burnett AP, inventors (1978). Leucite-containing porcelains and method of making same. US Patent 4101330.

Cattell MJ, Chadwick TC, Knowles JC, Clarke RL, Lynch E (2001). Flexural strength optimisation of a leucite reinforced glass ceramic. *Dent Mater* 17:21-33.

Cattell MJ, Chadwick TC, Knowles JC, Clarke RL (2005). The crystallisation of an aluminosilicate glass in the K_2O-Al_2O_3-SiO_2 system. *Dent Mater* 21:811-822.

Cattell MJ, Chadwick TC, Knowles JC, Clarke RL, Samarawickrama DY (2006). The nucleation and crystallisation of fine grained leucite glass-ceramics for dental applications. *Dent Mater* 22:925-933.

Conrad T, Meyer G, inventors (2007). Leucite glass ceramic doped with nanoscale metal oxide powder, method for producing the same, and dental materials and dental products formed therefrom. US Patent 7172649.

Cullity BD, Stock SR (2001). Elements of x-ray diffraction. 3rd ed. New Jersey: Prentice-Hall, pp. 439-441.

Davidge RW, Green TJ (1968). The strength of two-phase ceramic/glass materials. *J Mater Sci* 3:629-634.

Deer WA, Howie RA, Zussman J, Wise WS (2004). An introduction to rock-forming minerals. 2nd ed. Harrow, UK: Prentice-Hall, pp. 304-315.

Denry IL, Mackert JR, Holloway JA, Rosenstiel S (1996). Effect of cubic leucite stabilization on the flexural strength of feldspathic dental porcelain. *J Dent Res* 75:1928-1935.

Freiman SW, Onada GY, Pincus AG (1971). Spherulitic crystallization in glasses. In: *Advances in nucleation and crystallization in glasses.*

Hench LL, Freiman SW, editors. Columbus, OH: The American Ceramic Society, pp. 91-112.

Hermansson L, Carlsson R (1976). High and low temperature forms of leucite. In: *Proceedings of the Eighth International Symposium on the Reactivity of Solids*. Gothenberg, Sweden: Swedish Institute for Silicate Research, pp. 541-545.

Höland W, Frank M, Rheinberger V (1995). Surface crystallization of leucite in glasses. *J Non-Cryst Solids* 180:292-307.

Höland W, Rheinberger V, Schweiger M (2003). Control of nucleation in glass ceramics. *Phil Trans R Soc Lond: Math Phys Eng Sci* 361:575-589.

James PF (1982). Nucleation in glass-forming Systems. A review. In: *Advances in ceramics*. Nucleation and crystallization of glasses, 83rd Annual Meeting of the American Ceramic Society. Simmons JH, Uhlmann DR, Beall GH, editors. Washington, DC: The American Ceramic Society, pp. 14-48.

Lee HH, Kon M, Asaoka K (1997). Influence of modification of Na_2O in a glass matrix on the strength of leucite-containing porcelains. *Dent Mater J* 16:134-143.

Mackert JR (1988). Effects of thermally induced changes on porcelain-metal compatibility. In: *Perspectives in dental ceramics, proceedings of the Fourth International Symposium on Ceramics*. Preston JD, editor. Chicago: Quintessence Publishing Co., pp. 53-64.

Mackert JR, Twiggs SW, Russell CM, Williams AL (2001). Evidence of a critical leucite particle size for microcracking in dental porcelains. *J Dent Res* 80:1574-1579.

McLaughlin JR (1999). Bead size and mill efficiency–producing inorganic nanoparticles by milling with ultrafine ceramic beads. *Ceramic Industry* 149:34-40.

Metzler KT, Woody RD, Miller AW 3rd, Miller BH (1999). In vitro investigation of the wear of human enamel by dental porcelain. *J Prosthet Dent* 81:356-364.

Müller R, Zanotto ED, Fokin VM (2000). Surface crystallisation of silicate glasses: nucleation sites and kinetics. *J Non-Cryst Solids* 274:208-231.

Ota T, Takahashi M, Yamai I, Suzuki H (1993). High thermal expansion polycrystalline leucite ceramic. *J Am Ceram Soc* 76:2379-2381.

Palmer DC, Putnis A, Salje EKH (1988). Twinning in tetragonal leucite. *Phys Chem Miner* 16:298-303.

Pinckney LR, Beall GH (2008). Microstructural evolution in some silicate glass-ceramics: a review. *J Am Ceram Soc* 91:773-779.

Rouf MA, Hermansson L, Carlsson R (1978). Crystallisation of glasses in the primary phase field of leucite in the K_2O-Al_2O_3-SiO_2 system. *Trans J Br Ceram Soc* 77:36-39.

Schmelzer J, Pascova R, Möller J, Gutzow I (1993). Surface-induced devitrification of glasses: the influence of elastic strains. *J Non-Cryst Solids* 162:26-39.

Shareef MY, Van Noort R, Messer PF, Piddock V (1994). The effect of microstructural features on the biaxial flexural strength of leucite reinforced glass-ceramics. *J Mater Sci Mater Med* 5:113-118.

Timoshenko S, Woinowsky-Krieger S (1959). Theory of plates and shells. 2nd ed. New York: McGraw-Hill, pp. 70-71.

Tošić MB, Živanović VD, Grujić SR, Stojanovic JN, Nikolić JD (2008). A study of the primary crystallization of a mixed anion silicate glass. *J Non-Cryst Solids* 354:3694-3704.

Weinstein M, Katz S, Weinstein AB, inventors (1962). Fused porcelain-to-metal teeth. US Patent 3052982.

Wondraczek L, Pradeau P (2008). Transparent hafnia-containing b-quartz glass ceramics: nucleation and crystallization behavior. *J Am Ceram Soc* 91:1945-1951.

Zhang Y, Qu C, Rao PG, Lu M, Wu JQ (2007). Nanocrystalline seeding effect on the crystallisation of two leucite precursors. *J Am Ceram Soc* 90:2390-2398.

Zhang Y, Rao P, Lv M, Wu J (2008). Mechanical properties of dental porcelain with different leucite particle sizes. *J Am Ceram Soc* 91:527-534.

Zheng W, Cheng J, Tang L, Quan J, Cao X (2007). Effect of Y_2O_3 addition on viscosity and crystallization of the lithium aluminosilicate glasses. *Thermochim Acta* 456:69-74. To beaqui dolecaes enihit earum no